Univerzitet u Beogradu
Poljoprivredni fakultet
Institut za poljoprivrednu tehniku
Naučni časopis
POLJOPRIVREDNA TEHNIKA
Godina XLIX
Broj 2, 2024.
Strane: 82 – 104

University of Belgrade
Faculty of Agriculture
Institute of Agricultural Engineering
Scientific Journal
AGRICULTURAL ENGINEERING
Year XLIX
No. 2, 2024.
pp. 82 - 104

Original Scientific paper
Originalni naučni rad
DOI: 10.5937/PoljTeh2402082U

ENHANCING COOKING BANANA PRESERVATION: A MATHEMATICAL MODEL APPROACH

Muofunanya F. Umunna[*1]; S. A. Adzor[2]; D. F. Ikikiru[1]; O. Nyorere[1]; S. K. Chigbo[3]; E. T. Erokare[1]; A. B. Eke[3]

[1] *Department of Agricultural Engineering, Faculty of Engineering, Delta State University of Science and Technology, Ozoro, Nigeria*
[2] *Department of Materials and Metallurgical Engineering, Faculty of Engineering, Delta State University of Science and Technology, Ozoro, Nigeria*
[3] *Department of Agricultural and Bioresources Engineering, College of Engineering and Engineering Technology, Micheal Okpara University of Agriculture, Umudike, Nigeria*

Abstract: This study systematically investigated the solar drying kinetics of cooking banana slices with thicknesses of 5mm, 10mm, and 15mm at temperatures of 50°C, 60°C, and 70°C. Employing the solar drying method, the drying process exhibited a diffusion-controlled mechanism, transitioning from a brief constant rate period to a predominant falling rate period until reaching equilibrium moisture content. The drying rate constant (k) displayed an increasing trend with elevated temperature, while an inverse correlation was observed with slice thickness, establishing direct and inverse relationships with drying time and temperature, respectively.

Fifteen thin-layer drying models were applied to fit the moisture ratio (MR) data, and the Midilli-Kucuk model demonstrated superior performance, attributed to its high R^2 value (0.997) and lowest values of RMSE (0.00228) and X^2 (0.0000132).

Proven to be a robust tool, the Midilli-Kucuk model effectively predicted the single-layer drying kinetics of cooking banana slices, providing valuable insights for dryer design and processing.

Empirical equations derived from the obtained data enable the prediction of drying kinetics specifically for cooking banana slices in the solar drying method.

[*]Corresponding Author. Email address: umunnamuofunanya25@gmail.com
ORCID: 0000-0001-8737-2795

This study contributes significantly to the comprehension and optimization of the drying process for unripe cooking banana, offering practical implications for dryer design and processing enhancements.

***Key words**: Solar, drying, kinetics, cooking, banana, slices, Midilli-Kucuk, model*

INTRODUCTION

According to [1] and [2], cooking banana (*Musa* spp., ABB genome) originated from the hybridization of *Musa acumulata* and *Musa balbisiana*. Cooking banana fruits resemble unripe desert bananas, albeit larger in size than other banana cultivars. These cooking bananas are commonly consumed either raw, ripe, or cooked, while a portion is processed into stable products [2].

The introduction of cooking banana to southeastern Nigeria in the late 1990s by the International Institute of Tropical Agriculture (IITA) aimed to combat the black sigatoka disease. These bananas are nutritionally rich and have medicinal properties, particularly the flowers, which can be used to treat ulcer, dysentery, and bronchitis [3]. However, their high moisture content, ranging from 70-80% (wb) in ripe form, makes them vulnerable to post-harvest losses and weight loss during transportation [4].

Drying is a globally practiced food preservation method, reducing water content to prevent deterioration and microbial spoilage. Understanding the drying behaviour of agricultural products is crucial for equipment development and improvement. Mathematical modeling, based on the drying of thin layers of the product, plays a key role in simulating drying processes [5].

Mathematical modeling is essential for controlling the drying process and improving product quality. It helps study variables, predict drying kinetics, and optimize operational parameters. Various mathematical equations are used to describe agricultural product drying, with thin layer models being widely employed due to their simplicity [6]. Fick's second law is typically used to explain liquid diffusion, forming the basis for describing drying phenomena when employing thin-layer drying equations [7].

Numerous mathematical models have been applied to various agricultural products. These models are crucial for predicting effective drying times and temperatures, minimizing nutrient degradation [8]. However, there is limited research on the drying behaviour of cooking bananas, particularly during the water removal stage.

High moisture content in bananas, if not properly dried, leads to susceptibility to microbial attacks and substantial post-harvest losses. For example, India and Brazil have reported significant losses in banana production [9]. Cooking bananas are highly perishable, particularly when harvested unripe and green. Losses primarily result from poor handling, inadequate storage, and transportation options.

Drying is an effective alternative to extend the shelf life of cooking bananas. Modern drying methods aim to reduce energy consumption while maintaining product quality. Mathematical modeling of drying kinetics plays a pivotal role in this process. Drying kinetics vary for different agricultural products, and selecting the appropriate drying model is crucial.

Numerous models have been put forth to elucidate the moisture loss rate during the thin-layer drying of agricultural products, as demonstrated by [10].

The behavior of thin layers in this context hinges on how quickly moisture is transported from the material. This internal movement of moisture is governed by various physical mechanisms that act in different combinations. The choice of physical mechanisms for moisture movement is ultimately contingent on the nature of the product to be dried. Consequently, it is possible that the established models may not entirely suit the drying process for mangoes.

The study conducted by [11] proposed a straightforward model for moisture transfer in multi-dimensional products. In their research, they formulated the drying time for infinite slab products by establishing an analogy between heat diffusion and moisture transfer. This approach was further extended to multidimensional products by introducing geometric shape factors.

Understanding drying kinetics is pivotal in process modeling and design. However, the available data in the literature are often insufficient for comprehensive process design, making product-oriented experiments a common necessity. In the existing body of literature [12] introduced a widely recognized drying curve that encompasses two main phases: the constant drying rate period and the falling rate period. Nonetheless, it's worth noting that not all materials adhere to this specific pattern. In some cases, only the falling rate regions are observed.

The constant drying rate phase occurs when a film of water is readily available at the drying surface for evaporation into the surrounding medium. During this phase, the drying rate is akin to what occurs when a pool of water evaporates into the air. The rate is heavily influenced by factors such as air temperature, air humidity, and the efficiency of heat transfer to the water.

Conversely, the falling rate regions signify an increased resistance to both heat and mass transfer. This occurs when the surface water is depleted, and the moisture to be evaporated comes from within the material's structure, necessitating transport to the surface. Multiple falling rate regions suggest the potential for drying rates to be influenced by structural changes, such as case hardening and shrinkage.

Numerous studies have explored the thin layer drying method across a variety of agricultural products. Noteworthy examples include investigations into the drying of olive fruit [8], date palm [13], cocoa [14], potato mash [15], rapeseed [16], litchi [17], sorghum [18], hazelnuts [19], and finger millet [20]. Employing drying kinetics, coupled with chemical analysis, proves invaluable in forecasting optimal drying time and temperature combinations. This approach minimizes the degradation of nutritional parameters within the crop, enhancing overall efficiency.

The study's general objective is to identify a suitable thin layer drying model for cooking bananas. Specific objectives include investigating the effects of slice thickness, temperature, microwave power, and solar drying methods on cooking banana drying kinetics. Additionally, the study aims to determine effective moisture diffusivity and activation energy, as well as develop empirical prediction equations for oven, microwave, and solar drying methods.

The research is justified by the need to reduce post-harvest losses of cooking bananas and extend their shelf life. By understanding the drying kinetics, this study aims to improve food productivity, decrease losses, and enhance farmers' income. Proper drying techniques and mathematical modeling are essential for efficient post-harvest processing and preservation of agricultural products.

MATERIAL AND METHODS

2.1 Sample Collection and Preparation

A bunch of unripe cooking bananas (*Musa bluggoe*) as presented in Figure 1 was purchased from Ndoro Market in Umuahia, Abia State. The selection of these bananas was based on their availability, as well as their medicinal and nutritional properties. Banana fingers were chosen based on their appearance and size, ensuring there was no evidence of mechanical damage. Afterward, they were detached, peeled, washed, and sliced into various thicknesses (5 mm, 10 mm, and 15 mm), using a sharp stainless steel knife. The slice thickness was determined with a digital vernier caliper with a sensitivity of 0.01mm.

Figure 1. Cooking banana

Experimental Procedure for Solar Drying

An active solar drying apparatus, situated within the Department of Agricultural and Bio-resources Engineering, as depicted in Figure 2, was utilized. The solar drying system incorporated key components, including a solar collector, an 180W capacity solar panel, a DC blower fan, a drying chamber, heat storage unit, drying trays, and a 200Ah rated solar battery. The solar dryer, featuring a transparent cover made of perplex material, demonstrated efficient utilization of solar energy. The 180W solar panel charged the DC battery, powering the intelligently programmed control box. This control box regulated the DC blower at intervals, responding to moisture levels within the drying chamber. Within the drying chamber, products undergoing drying were positioned on perforated metal trays, facilitated by a convenient door for easy tray insertion and removal. A heat storage unit, containing black pebbles, effectively harnessed and stored solar energy for sustained use. Positioned atop the dryer, a blower directed air from the inlet opening through a solar collector chamber, passing through the product bed. Solar radiation, captured by the system, heated the air flowing through the drying product.

The heated air traversed the drying chamber, and at its zenith, vents facilitated the removal of moisture.

Figure 2. Active solar drying device

Design of Experiment

The experiments were carried out following a factorial design, comprising two factors, each with three levels. This resulted in a 2x3 factorial design (2 factors, 3 levels each). The independent parameters for the research study were temperature and thickness. Temperature was classified into three levels, denoted as T1, T2, and T3, whereas thickness was delineated by three levels: t1, t2, and t3. To ensure robustness and reliability, these experiments were replicated thrice, and the average values were employed for subsequent calculations.

Factorial design for solar drying

Table 1 presents the combinations of thickness (5 mm, 10 mm, and 15 mm) with corresponding experiments for solar drying. It also provides a clear overview of the combinations of thickness and drying method used. Thus serving as a valuable reference for understanding the factorial design implemented in the study.

Table 1. Factorial Design Experiments for Solar Drying at Various Thickness Levels.

Thickness (mm)	Solar
5	Experiment 1
10	Experiment 2
15	Experiment 3

Moisture Content Determination

The initial moisture content of the cooking banana slices was assessed using a Mermet oven set at 105ºC for 24 hours until a constant weight was achieved, following the method outlined by [21]. The experiment was meticulously replicated to ensure precision. Moisture content on a wet basis was calculated using Equation 1.

$$Mc\ (w.b)\ \% = \frac{\boldsymbol{Ww - Wd}}{\boldsymbol{Ww}} \boldsymbol{x} \frac{\mathbf{100}}{\mathbf{1}} \qquad \ldots\ldots\ldots\ldots\ldots\ldots \qquad (1)$$

Where:
Mc = (W.b) moisture content at wet basis,
Ww = weight of wet sample (g),
Wd = weight of dried sample (g)

Determination of Moisture Ratio (MR)

The moisture ratio (MR) for the cooking banana was determined using Equation 2, as proposed by [22].

$$MR = \frac{Mt - Me}{Mo - Me} \quad \text{…… (2)}$$

Subsequently, the moisture ratio was further simplified in accordance with the methodology outlined by [23] as expressed in Equation 3.

$$MR = \frac{Mt}{Mo} \quad \text{…… (3)}$$

Where:
Mt= Moisture content at any time (t),
Mo = Initial moisture content,
Me = Equilibrium moisture content

All values are expressed as grams of water per gram of dry matter. The values of Me were determined as the moisture content at the conclusion of the drying process when the sample ceased to lose mass.

Drying Rate Calculation (DR)

The drying rate was determined following the formulation provided by [24], [25], and [26] in Equation 4.

$$D_r = \frac{M_{t+dt} - M_t}{dt} \quad \textbf{……..(4)}$$

Where:
M_t = moisture content at a specific time (g water g dry base-1),
M_{t+dt} = moisture content t+dt (g water g dry base-1),
t = drying time (hr)

Determination of Effective Moisture Diffusivity

The effective moisture diffusivity (D_{eff}) was calculated using a lumped parameter approach, considering all potential resistances to moisture transport. For an infinite slab in one dimension, assuming negligible temperature gradient within the product, constant temperature and diffusivity, and no significant external resistance, moisture transfer during the falling-rate drying period was determined using Fick's Second law, as expressed in Equation 5, [27].

$$MR = \frac{8}{\pi^2} \sum_{n=0}^{\infty} \left(\frac{1}{2n+1}\right) \exp\left(-\frac{(2n+1)^2 \pi^2 D_{eff} t}{4L^2}\right) \quad \text{…… (5)}$$

Where:
MR is the moisture ratio,
D_{eff} = effective diffusivity (m^2/s)
Mt = the moisture content at any time (Kg water /kg dry matter),
n = 1, 2, 3 -------- the number of term taken into consideration,
t = the time of drying in seconds, *l* =the thickness of slice (m)

Equation 5 is further simplified as shown in Equation 6, 7, and 7 respectively in line with [28].

$$MR = \frac{8}{\pi^2} \exp\left[\frac{\pi^2 D_{eff} t}{4L^2}\right] \quad \text{……(6)}$$

$$MR = \frac{8}{\pi^2} \exp(-kt) \quad \text{…… (7)}$$

The slope k is calculated by plotting *In(MR)* versus time

$$K = \frac{\pi^2 D_{eff}}{4l^2} \quad \text{… … … … … … … … … (8)}$$

Determination of the Activation Energy
Temperature has a significant impact on diffusivity, and to quantify this effect, the Arrhenius Equation 9 was utilized. Higher activation energy indicates greater sensitivity to temperature [29]. Taking the natural logarithm of Equation 9 reveals a linear relationship between the natural log of diffusivity and temperature. In cases where a robust correlation cannot be established, it suggests that external factors strongly influence effective diffusivity [30]. To account for these effects, a mathematical relationship must be proposed and tested using non-linear regression.

$$D_{eff} = Do \exp\left(\frac{-Ea}{R(T+273.15)}\right) \quad \text{….. (9)}$$

Where:
Ea = energy of activation ($kJmol^{-1}$),
R = the universal gas constant ($8.3143Jmol^{-1}KJmol^{-1}KJmol^{-1}$),
T = absolute temperature of the drying medium (K),
Do = line intercept, which is always constant .

The linear form equation, derived through the application of logarithmic operations, is presented in Equation 10.

$$InD_{eff} = InDo \exp\left(\frac{-Ea}{R(T+273.15)}\right) \quad \text{…… (10)}$$

Mathematical Modelling of Drying Kinetics

To comprehensively investigate the drying kinetics of agricultural commodities, effective modeling of drying behaviour becomes indispensable. Data acquired from the experimental drying of cooking banana at various temperatures and thicknesses were subjected to fitting with fifteen thin-layer drying mathematical models proposed by various authors, as detailed in Table 2. The curve fitting process utilized [31] the Microsoft Excel (2016) Solver add-ins.

Statistical Evaluation of Drying Models

Relevant statistical parameters were employed to discern the most suitable drying equation/model that accurately represents the drying curves of the samples, and to assess the validity of the fits. The least square method of parameter estimation, as outlined by [32], was applied to ascertain the missing parameters of the drying models.

The coefficient of determination (R^2), the reduced chi-square value, an (x^2)d root mean square error (RMSE), as expressed in Equations 11, 12, and 13, were employed for the selection of the optimal equation that captures the drying curves of the sample.

The determination of the best fit relied on identifying the highest values of R^2 and the lowest values of X^2, in accordance with the criteria established by [33] and [34].

After determining the unknown parameters, the model underwent validation through a comprehensive comparison of experimental data and predicted data to ensure consistency.

$$R^2 = \frac{\sum_{i=1}^{N} MR_{Pre,i} MR_{exp,i} - \sum_{i=1}^{N} MR_{pre,i} \sum_{i=1}^{N} MR_{exp,i}}{\sqrt{(\sum_{i=1}^{N} (MR_{pre,i})^2 - (\sum_{i=1}^{N} MR_{pre,i})^2)(N\sum_{i=1}^{N} MR_{exp,i} - (\sum_{i=1}^{N} MR_{exp,i})^2)}} \quad \textbf{.....(11)}$$

Where:

$MR_{exp,i}$ (experimental moisture ratio),

$MR_{pre,i}$ (predicted moisture ratio),

n is the number of constants, and

N is the number of observations.

$$X^2 = \frac{\sum_{i=1}^{n} (MR_{exp,i} - MR_{pre,i})^2}{N-n} \quad \textbf{.....(12)}$$

$$\textbf{RMSE} = \left[\sum_{i=1}^{N} \frac{1}{N} (MR_{exp,i} - MR_{pre,i})^2\right]^{\frac{1}{2}} \quad \textbf{... (13)}$$

Table 2. Thin layer mathematical models used

No	Model name	Model Equation	Reference
1	Newton	MR = exp (-kt)	Mujumdar (2006)
2	Page	MR = exp ($-kt^n$)	Flores et al. (2012)
3	Modified Page	MR = exp[$-(kt)^n$]	Demir et al. (2007)
4	Henderson and Pabis	MR = a exp ($-kt^n$)	Radhika et al.(2011)
5	Modified Henderson and Pabis	MR = a exp(−kt) + b exp(−gt) + c exp(−ht)	Zenoozian et al. (2008)
6	Midilli and Kucuk	MR = a exp($-kt^n$) + bt	Midilli and kucuk (2002)
7	Modified Midilli	MR = a exp(−kt) + b	Gan and Poh (2014)
8	Logarithmic	MR = a exp (-kt)+c	Yagcioglu et al. [1999]
9	Two-term	MR = a exp($-K_1t$) + b exp ($-K_2t$)	Sacilik (2007)
10	Two-term exponential	MR = a exp($-k_0t$) + (1 – a)exp ($-k_1at$)	Dash et al. (2007)
11	Demir et al.	MR = a exp ($-K\ t)^n$ + b	Demir et al. (2007)
12	Verma et al.	MR = a exp(−kt) + (1 − a)exp (−gt)	Akpinar (2006)
13	Approximation of diffusion	MR = a exp(−kt) + (1 − a) exp (−kbt)	Yaldyz and Ertekyn (2007)
14	Hii et al.	MR = a exp($-K_{\ 1}t^n$) + b exp($-K_{\ 2}t^n$)	Kumar et al. (2014)
15	Wang and Singh	MR = $1+at+bt^2$	Radhika et al. (2011)

Where: MR = (M – Me)/(Mo – Me),
Moisture ratio (dimensionless); a, b, c, g, h, k, k_0, k_1, k_2,
n = drying constants,
t = drying time (min).

RESULTS AND DISCUSSION

Influence of Temperature on Moisture Content Removal

In Figures 3-5, a discernible trend emerges as an escalation in drying temperature correlates with an augmented drying rate, consequently leading to a reduction in overall drying time. This phenomenon is attributed to the inherent relationship between drying temperature and the associated driving force for heat transfer. As elucidated by [35], higher drying temperatures engender a more substantial water vapour pressure deficit, defined as the variance between saturated water vapour pressure and the partial pressure of water vapour in air at a given temperature.

This differential pressure represents a pivotal driving force influencing the efficiency of the drying process. The findings presented herein align with prior research, notably the work of [35], and are congruent with observations reported by [36]. The study establishes that elevated drying temperatures contribute to an intensified water vapour pressure deficit, thereby expediting the overall drying kinetics. Moreover, the investigation discerns that the duration required to reduce the initial moisture content to a predetermined level is contingent upon various drying conditions.

Specifically, the drying time exhibits an inversely proportional relationship with temperature, with the longest duration observed at 50°C and the shortest at 70°C.

Furthermore, the thickness of the material plays a crucial role, with the drying period extending for the maximum duration at a thickness of 15mm and contracting to the minimum at 5mm. These nuanced findings underscore the interplay of temperature and thickness in shaping the dynamics of the drying process.

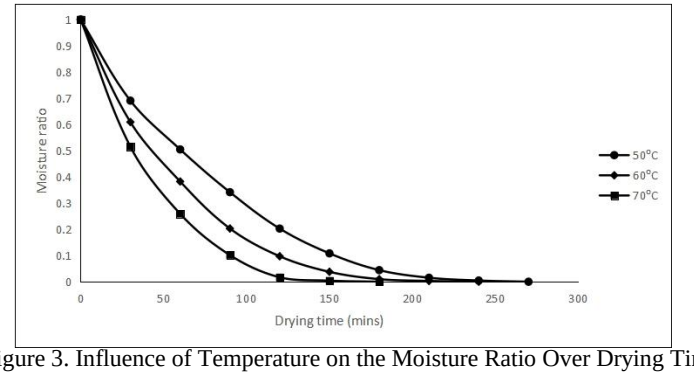

Figure 3. Influence of Temperature on the Moisture Ratio Over Drying Time at a Slice Thickness of 5 mm

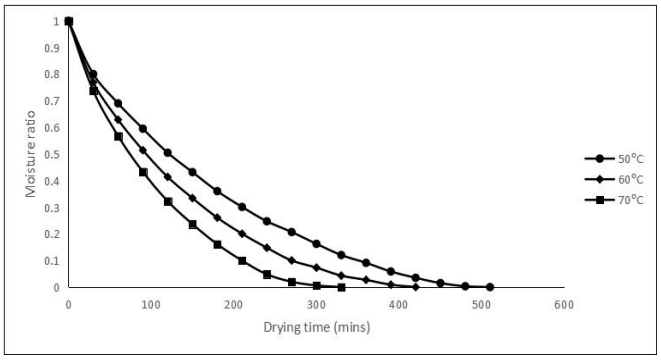

Figure 4. Influence of Temperature on the Moisture Ratio Over Drying Time at a Slice Thickness of 10 mm

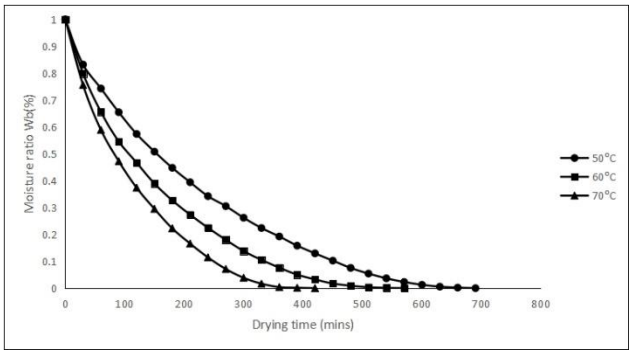

Figure 5. Influence of Temperature on the Moisture Ratio Over Drying Time at a Slice Thickness of 15 mm

Influence of Slice Thickness on the Moisture Ratio Variation over Drying Time

The graphical representation in Figures 6-8 underscores a discernible correlation between slice thickness and drying time. Notably, there is a conspicuous increase in drying time as the slice thickness augments. Conversely, a continuous decrease in drying time is evident as moisture content diminishes.

This observation signifies that the drying process experiences a substantial reduction in time as it nears the initial moisture content. The inverse relationship between drying time and moisture content is particularly noteworthy, implying that the duration required for the material to reach a certain moisture level diminishes significantly as it approaches the initial moisture content.

Furthermore, the data elucidates that sample thickness is a pivotal factor influencing drying time, with higher thicknesses correlating with prolonged drying periods.

In essence, these findings emphasize the critical impact of both slice thickness and moisture content on the kinetics of the drying process. As slice thickness increases, so does the drying time, while a decrease in moisture content is associated with a notable reduction in the time required for the material to attain its specified moisture level. This nuanced understanding contributes valuable insights into the intricate dynamics governing the drying behaviour under different thickness and moisture content condition.

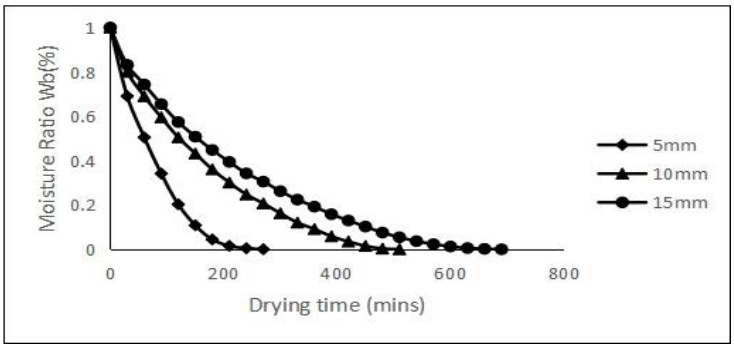

Figure 6. Influence of Slice Thickness on the Moisture Ratio Variation Over Drying Time at 50°C

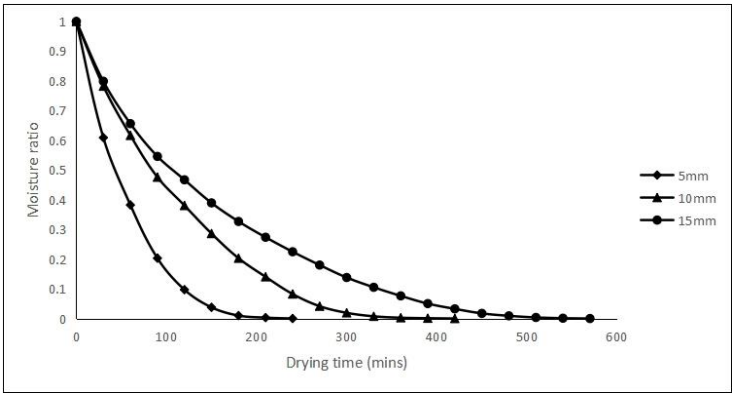

Figure 7. Influence of Slice Thickness on the Moisture Ratio Variation Over Drying Time 60ºC

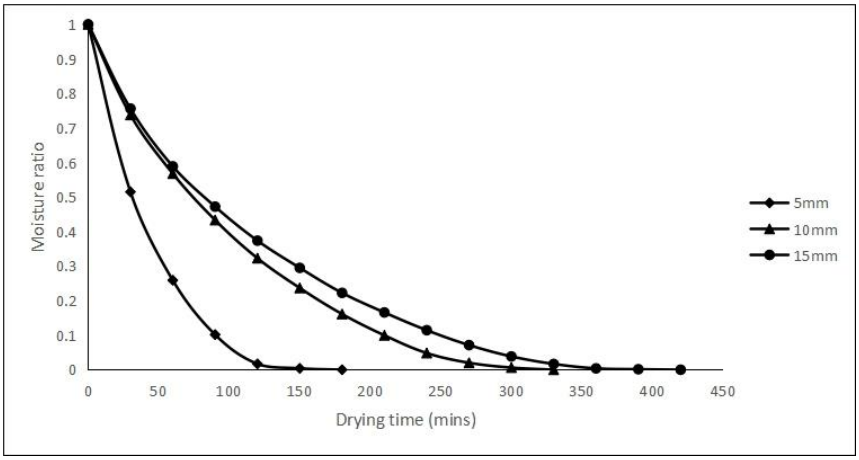

Figure 8: Influence of Slice Thickness on the Moisture Ratio Variation Over Drying Time 70ºC

Impact of Drying Rate on Drying Time at Various Temperatures

In Figures 9-11 the drying rate profiles are illustrated with respect to time, encompassing various thicknesses and temperatures. The determination of drying rate involved the computation of the time required to eliminate a specified quantity of moisture from the drying samples. Notably, the drying rate exhibited a diminishing trend concomitant with an increase in both drying time and temperature. This decline in drying rate during the process is indicative of a reduction in moisture migration from the interior to the surface of the product. The observed behavior of the drying rate manifests in both constant and falling rate periods. Initially, the drying rate was notably high, corresponding to the elevated moisture content in the samples. As the drying process advanced towards the falling rate period, the drying rate gradually decreased until reaching a state of constancy, marking the attainment of the equilibrium moisture content stage. This dynamic aligns with prior studies, as evidenced by [37] in the context of onion slices [38] for parboiled wheat, and [39] in the case of green beans. The parallel trends observed in the current investigation substantiate the broader applicability of these findings across diverse drying scenarios.

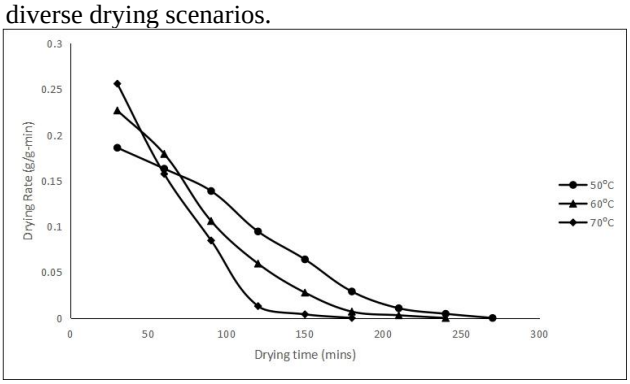

Figure 9. Impact of Drying Rate on Drying Time at Various Temperatures for slice thickness of 5mm

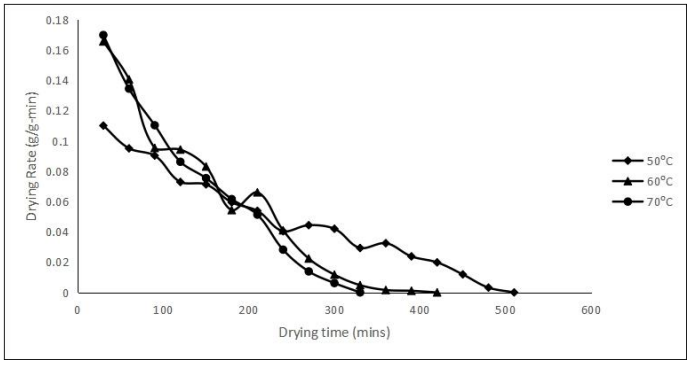

Figure 10. Impact of Drying Rate on Drying Time at Various Temperatures for slice thickness of 10mm.

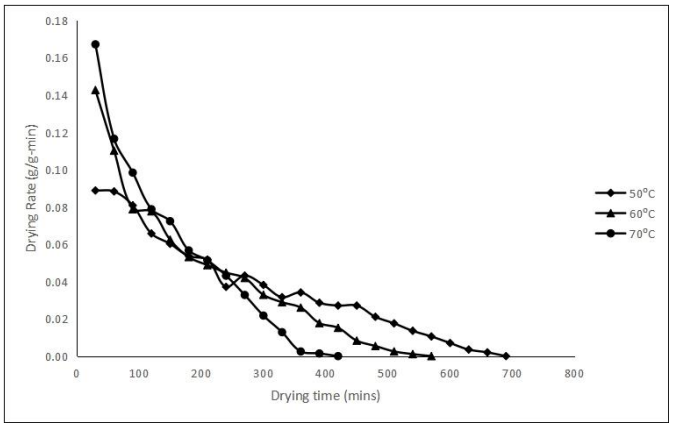

Figure 11. Impact of Drying Rate on Drying Time at Various Temperatures for slice thickness of 15mm

Impact of Temperature and Slice Thickness on Drying Time

The graphical representation of drying temperatures against drying duration is depicted in Figure 12. Notably, the observed trends indicate a substantial influence of slice thickness and drying temperature on the drying time of the product. Examining specific combinations, it becomes evident that the product characterized by the lowest thickness (5mm) and the highest temperature (70°C) manifests the briefest drying duration, recording a mere 180 minutes. Conversely, the product featuring the highest thickness (15mm) coupled with the lowest temperature (50°C) results in the lengthiest drying period, totaling 690 minutes.

These findings elucidate a direct correlation between drying time and temperature, wherein higher temperatures correspond to shorter drying durations. Conversely, a distinct inverse relationship is observed between drying time and slice thickness, where thinner slices correlate with briefer drying periods.

This nuanced understanding enhances our comprehension of the interplay between temperature, slice thickness, and drying time, providing valuable insights for optimizing the drying process in various scenarios.

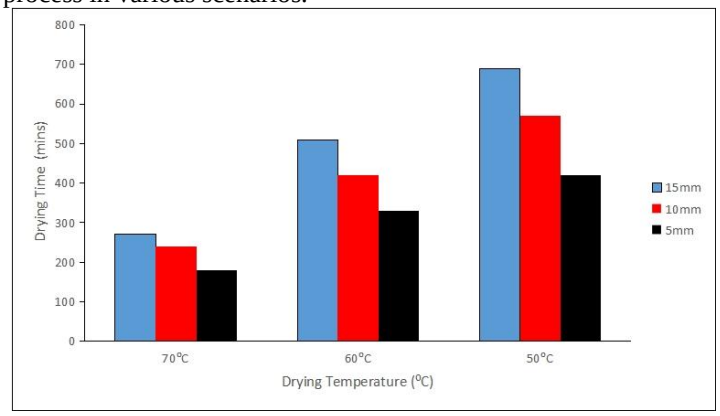

Figure 12. Impact of Drying Temperature on Drying Time

3.5 Drying rate constant (K)

The determination of the drying rate constant involves a methodical approach, achieved by plotting the natural logarithm of the moisture ratio (ln MR) against time (t). This analytical process is elucidated through the graphical representations in Figures 13-15. The rationale behind employing the natural logarithm lies in its ability to transform the moisture ratio data into a linear format when plotted against time. The resulting plots exhibit a linear relationship, and through this transformation, the drying rate constant (K) can be precisely determined. The logarithmic transformation facilitates the generation of a straight-line graph, and the slope of this line corresponds to the drying rate constant under the specific conditions prevailing during the drying process.

In essence, Figures 13-15 capture the crucial step of estimating the drying rate constant by leveraging logarithmic transformation, providing a visual depiction of the relationship between ln MR and time. This approach not only enhances the precision of the determination but also allows for a comprehensive understanding of the drying kinetics at the given set of conditions.

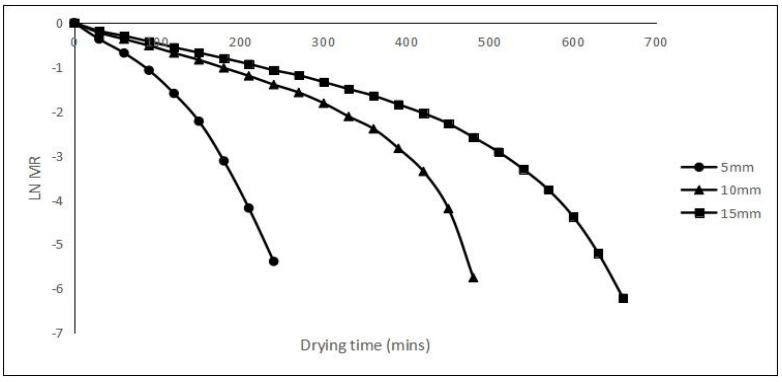

Figure 13. Logarithm of Moisture Ratio for Slice Thicknesses of 5mm, 10mm, and 15mm in Relation to Drying Temperature at 50°C

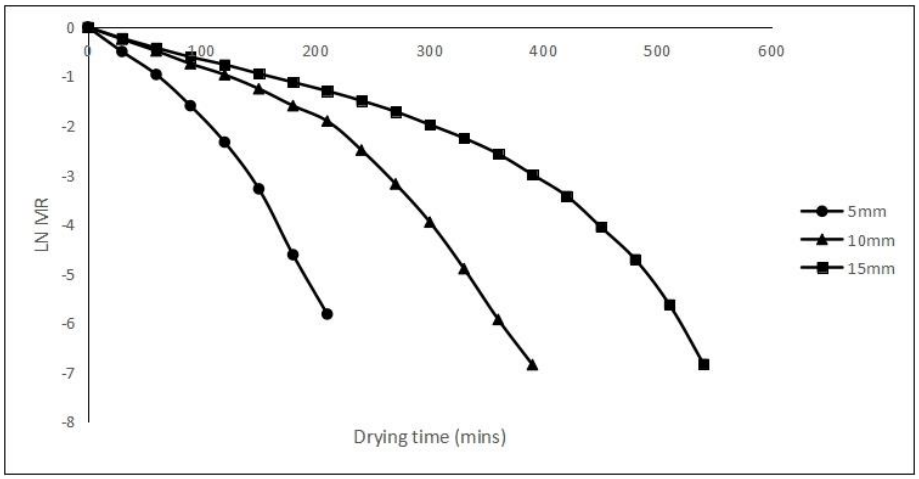

Figure 14. Logarithm of Moisture Ratio for Slice Thicknesses of 5mm, 10mm, and 15mm in Relation to Drying Temperature at 60°C

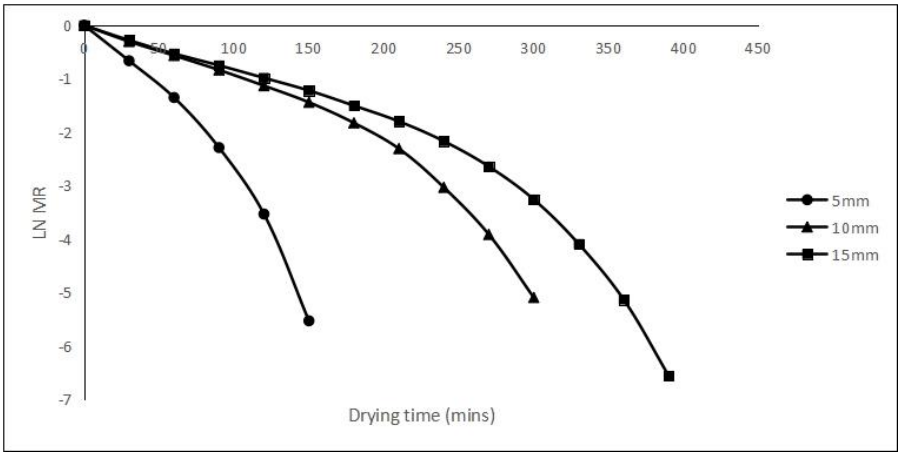

Figure 15. Logarithm of Moisture Ratio for Slice Thicknesses of 5mm, 10mm, and 15mm in Relation to Drying Temperature at70°C

Kinetics of Solar Drying

Figures 16-19 present the drying curves for cooking banana slices with thicknesses of 5mm, 10mm, and 15mm during solar drying. The drying process revealed distinct phases, characterized by short constant and extended falling rate periods. In Figure 16 the drying rate curves depict a notable decrease in drying rate with increasing sample thickness.

This observation aligns with the trend of increased drying time at higher sample thickness, a phenomenon attributed to the diminished drying rate. Similar findings have been reported in previous studies [40] and [41].

Figures 18-19 provide a comprehensive overview of the drying measurements and parameters recorded during the course of the drying durations for 5mm, 10mm, and 15mm sample thicknesses.

An examination of the drying chamber temperature reveals a peak around midday (12:00 pm), consistently surpassing ambient temperature levels. Solar intensity is shown to peak between 11:30 am and 2:00 pm, followed by a gradual decline. Relative humidity exhibits an inverse relationship with drying chamber and ambient temperatures, decreasing sharply during the noon period due to the heating of air. Wind speed demonstrates higher levels during the afternoon and evening compared to the early morning.

The increase in drying rate is observed to coincide with the rise in solar intensity, with the maximum drying rate occurring between 12:00 pm and 2:00 pm. This peak aligns with the drying chamber reaching its maximum temperature, as illustrated in Figures 18-19. These detailed observations offer valuable insights into the intricate interplay of environmental factors and their impact on the solar drying kinetics of cooking banana slices.

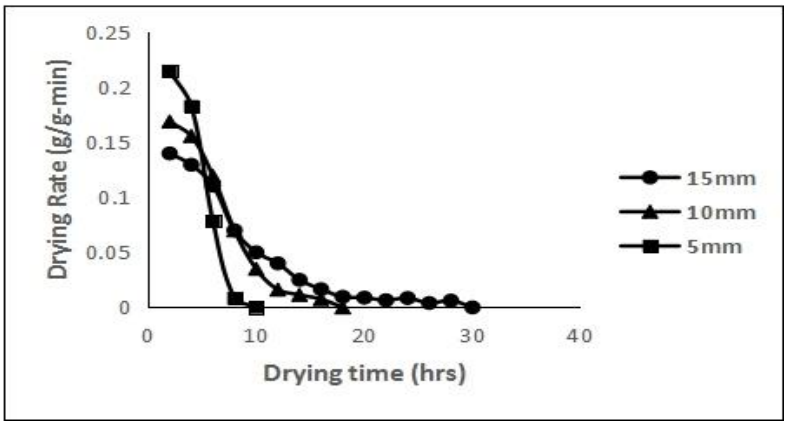

Figure 16. Solar drying rate for cooking banana

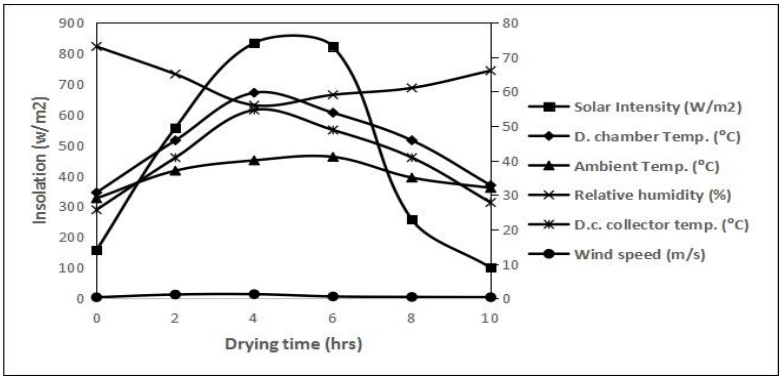

Figure 17. Solar drying parameter values for thickness of 5mm

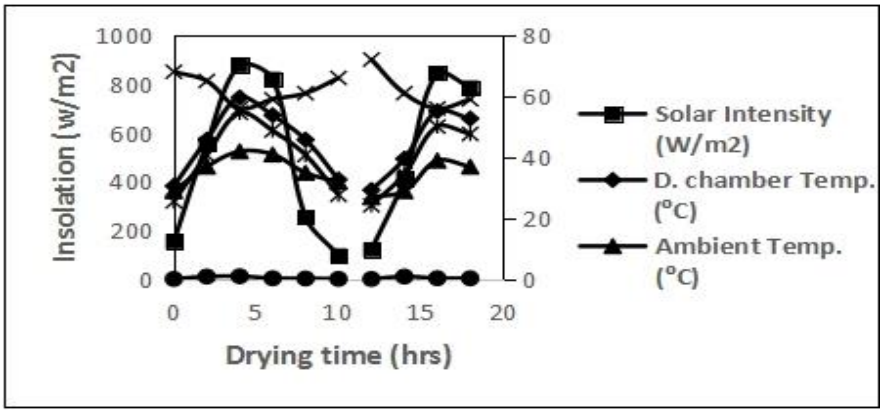

Figure 18. Solar drying parameter values for thickness of 10mm

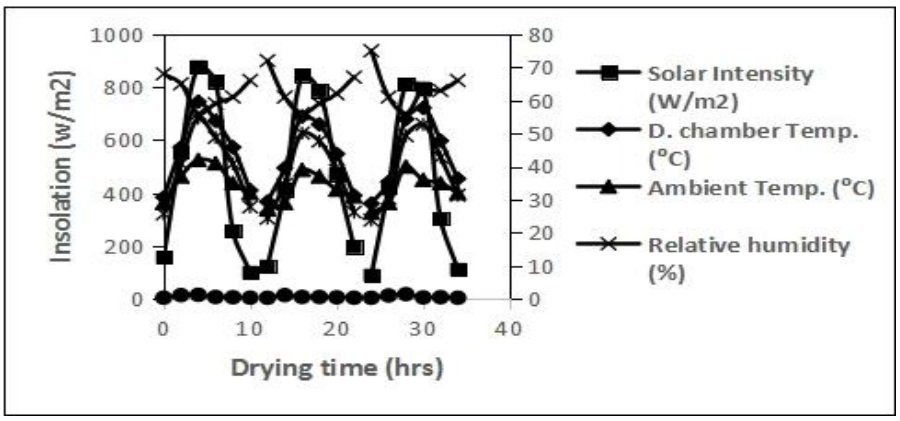

Figure 19. Solar drying parameter values for thickness of 15mm

Modeling Solar Drying Kinetics for Cooking Banana Slices

Table 3 provides a comprehensive overview of the statistical outcomes derived from the non-linear regression analysis conducted on the experimental data of solar drying, employing the moisture ratio as a key parameter. The validation of the best-fitted model was meticulously undertaken through both statistical and graphical assessments.

In tandem, Table 4 presents the outcomes of the non-linear regression analysis for the best-fitting model, elucidating the chosen model's conformity to the experimental data. Various criteria were employed to evaluate the goodness of fit, including the highest R^2 value, the lowest RMSE, and the reduced chi-square (X^2).

Following a rigorous assessment based on these criteria, the model proposed by Midilli and Kucuk emerged as the most appropriate representation for the single-layer drying behaviour of cooking banana slices in solar drying processes. This selection was made due to its superior alignment with the experimental data and its notable performance in terms of statistical metrics.

Table 3. Statistical Analysis of Selected Drying Models for Solar

		Solar		
No	Model Name	R^2	X^2	RMSE
1	Newton	0.969	0.000276	0.0126
2	Page	0.968	0.00405	0.0513
3	Modified Page	0.968	0.00405	0.0513
4	Henderson and Pabis	0.960	0.00147	0.0305
5	Modified Henderson and Pabis	0.985	0.00624	0.05517
6	Midilli and Kucuk	0.997	0.0000132	0.00228
7	Modified Midilli	0.991	0.0000236	0.004
8	Logarithmic	0.987	0.0000406	0.00493
9	Two-term	0.944	0.00544	0.0537
10	Two-term exponential	0.944	0.00483	0.0537
11	Demir *et al.*	0.987	0.0000523	0.00493
12	Verma *et al.*	0.989	0.00213	0.0375
13	Approximation of diffusion	0.944	0.005	0.054
14	Hii *et al.*	0.961	0.002	0.029
15	Wang and Singh	0.917	0.0663	0.22249

Table 4. Statistical Analysis of the Midilli and Kucuk Model for Solar Drying

	t(mm)	N	A	$K(min)^{-1}$	B	R^2	X^2	RMSE
	5	1.175	1.0023	0.00373	0.0006168	1.000	1.89E-07	0.00034
Solar	10	1.258	1.0091	0.003044	0.0007628	0.999	2.61E-06	0.00125
	15	0.993	1.0401	0.007397	0.0004546	0.993	3.69E-05	0.00526
	Mean	1.142	1.0172	0.00472	0.000611	0.997	1.32E-05	0.0023

Validation of the Selected Model

The validation of the statistical results for the Midilli and Kucuk model was conducted through a meticulous comparison of experimental moisture ratio (MR) and predicted moisture ratio (MR) data.

The validation process involved plotting the predicted MR values against the corresponding experimental MR values, as illustrated in Figures 20-22. The graphical representation clearly indicates the proximity of the predicted MR values to the linear trend of the graph, affirming the reliability of the selected model.

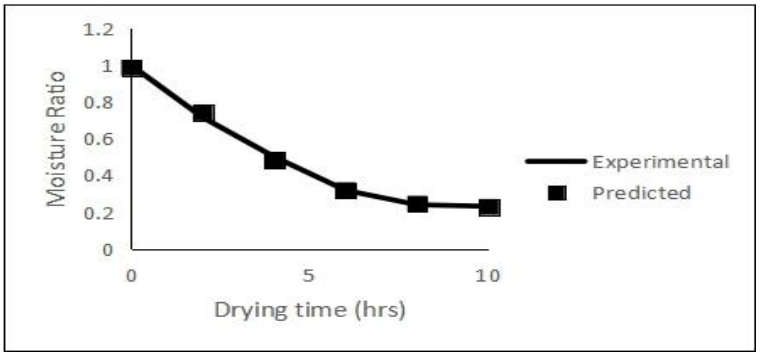

Figure 20. Comparison of experimental and predicted moisture ratio values by Midilli and Kucuk model for 5mm thickness for solar drying

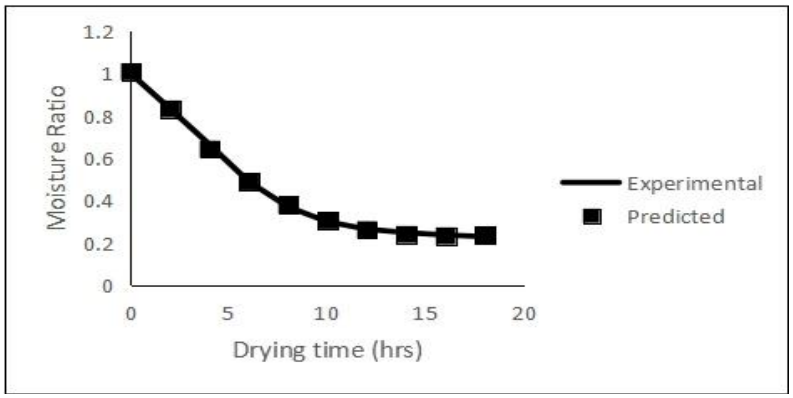

Figure 21. Comparison of experimental and predicted moisture ratio values by Midilli and Kucuk model for 10mm thickness for solar drying

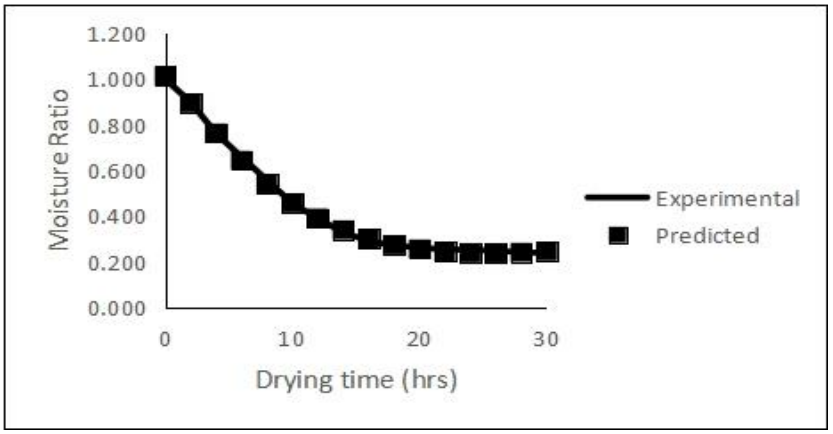

Figure 22. Comparison of experimental and predicted moisture ratio values by Midilli and Kucuk model for 15mm thickness for solar drying

Considering the constants, coefficients, and factors of the Midilli and Kucuk drying model for solar drying, successful prediction of the moisture ratio for cooking banana slices with thicknesses of 5mm, 10mm, and 15mm at different drying stages (t) within the temperature range of (50-70 ^{o}C) can be achieved using the following equations.

$$5mm;\ MR = 1.002\ Exp\ (-3.73E^{-3}xt^{1.175}) + 6.168E^{-4}t \quad \ldots\ldots\ldots (14)$$

$$10mm;\ MR = 1.009\ Exp\ (-3.04E^{-3}xt^{1.258}) + 7.628E^{-4}t \quad \ldots\ldots\ldots (15)$$

$$15mm;\ MR = 1.040\ Exp\ (-7.40E^{-3}xt^{0.993}) + 4.546E^{-4}t \quad \ldots\ldots\ldots (16)$$

CONCLUSIONS

In light of the findings from the research study, the ensuing conclusion emerges:

1. The findings underscored that the drying mechanism for cooking banana follows a diffusion-controlled process. Commencing with a brief constant rate period, the predominant drying occurred during the falling rate period, culminating with the attainment of the equilibrium moisture content threshold (EMC).
2. Drying rate constant (k) exhibited an upward trend with increasing drying temperature, while it decreased in tandem with an increase in slice thickness. Succinctly, this implies a direct relationship between drying time and slice thickness, coupled with an inverse correlation with drying temperature.
3. Fifteen thin-layer drying models were employed to fit the drying data (MR), and their validity was assessed through coefficients of determination (R^2), root mean square error (RMSE), and reduced chi-square (X^2) parameters. The Midilli-Kucuk model emerged as the most adept in elucidating the single-layer drying kinetics across diverse experimental conditions, outperforming alternative model for solar drying scenario due its high R^2 value, and lowest values of RMSE and X^2.
4. These results establish the efficacy of the Midilli-Kucuk model as a robust tool for predicting the single-layer drying kinetics of cooking banana slices, serving as a valuable asset in the design of dryers and processing of unripe cooking banana. Empirical equations were formulated based on the obtained data to facilitate the prediction of drying kinetics for cooking banana slices in solar drying method.

REFERENCES

[1] Stover, R.H. and N.W., Simmonds.1987. Bananas (Tropical Agriculture). Third Edition New york: John Wiley and Sons, Inc. Longman Scientific andTechnical publishers.
[2] Robinson, J.C. 1996. Bananas and Plantains. Crop Production Science in Horticulture. (5). CAB International, Wallingford, U.K.
[3] Raynold, L. T. 2003. The global banana trade. In book:Banana wars, pp. 23-47.
[4] Valmayor, R.V., Jamaluddin, S.H., Silayoi, B. 2000. Banana cultivar names and synonyms in Southeast Asia. In: Proceedings of International Network for the Improvement of Banana and Plantain – Asia and the Pacific Office, pp. 24. Philippines: Los Banos, Laguna.

[5] Berbert, P. A, Queiroz, D. M, Silva, J. S., Pinheiro Filho J. B.1995. Simulation of Coffee Drying in a Fixed Bed with Periodic Airflow Reversal. Journal of Agricultural Engineering Research, 60, (3): pp.167-175
[6] Geetha, P., Bhavana, M., Krishna Murthy, T. P., Krishna Murthy, N. B. and Ananda, S. 2014. Microwave Drying of Sprouted Horse Gram (Macrotyloma Uniflorum): Mathematical modeling of drying kinetics. *Research Journal of Recent Sciences*, 3(8):pp.96-102.
[7] Doungporn, S., Poomsa-ad, N. and Wiset, L. 2012. Drying equations of Thai Hom Mali paddy by using hot air, carbon dioxide and nitrogen gases as drying media. *Food Bioproduction Processing*, 90(1): pp.187–198.
[8] Mahdhaoui, B., Mechlouch, R. F., Mahjoubi, A., Zahafi, K. and Brahim, A. B. (2013). Mathematical model on thin layer drying of olive fruit (Olea *europeae). Journal of Agricultural Technology*, 9(5): pp.1097-10.
[9] Food and Agriculture Organization of the United Nations, 2011. Statistical databases. Rome, Italy. http://www.fao.org (accessed June, 2020).
[10] Bakker-Arkema, L.W., Lerew, L.W., DeBore, S.F. and Roth, M.G.1984. Grain drying simulation. Research Report, Michigan State University, Agricultural Experiment Station.
[11] Sahin, A. Z., Dincer, I., Yilbas, B. S. and Hussain, M. M. 2002. Determination of drying times for regular multi-dimensional objects. *International Journal of Heat and Mass Transfer*.1(45): pp.1757–1766.
[12] Mujumdar, A.S. (Ed.), 1995, Handbook of Industrial Drying, 2nd Edition, M. Dekker, N.York.
[13] Darvishi, H. and Hazbavi, E. (2012). Mathematical modeling of thin-layer drying behaviour of date palm. *Glob J Sci Front Res Math Dec Sci*, 12(10): pp.9–17.
[14] Hii C. L., Law C. L., and Cloke M. 2008. Modeling of Thin Layer Drying Kinetics of Cocoa Beans during Artificial and Natural Drying. *Journal of Engineering Science and Technology*. 3(1): pp.1-10.
[15] Goyal, S., Kumar, M. and Kaur, A.2014. Thin Layer Drying Kinetics of Potato Mash. *Int. Journal of Management, Information Technology and Engineering*,2(1): pp.43-56.
[16] Duc, L. A., Han J. W. and Keum, D. H. 2011. Thin layer drying characteristics of rapeseed (Brassica napus L.). *Journal Stored Product Res*. 47(1): pp.32-38.
[17] Janjai, S., Precopped, M., Lamlerta, N., Mahayotheeb, B., Balac, B. K., Nagle, M. and Müllerd, J. 2011. Thin layer drying of litchi (Litchi *chinensis Sonn*.). *Food Bio-production Process*, 89(1): pp.194-201.
[18] Shen, F., Peng, L., Zhang, Y., Wu, J., Zhang, X., Yang, G., Peng, H., Q, H. and Deng, S. 2011. Thin-layer drying kinetics and quality changes of sweet sorghum stalk for ethanol production as affected by drying temperature. Ind. Crops Prod. 34: pp.1588- 1594.
[19] Ozdemir, M. and Devres, Y. O. 2000. The thin layer drying characteristics of hazelnuts during roasting. *Journal of Food Engineering*, 42(1): pp.225-233.
[20] Radhika, G. B., Satyanarayana, S. V. and Rao, D. G. 2011. Mathematical Model on Thin Layer Drying of Finger Millet (*Eluesine coracana*). *Advanced Journal of Food Science Technology*, 3(2): pp.127-131.
[21] Association of Official Analytical Chemist 2000. Official method of analysis. No.920.149149(c).17th ed. Horwitz, USA.
[22] Babalis, S.J. and Belessiotis, V.G. 2004. Influence of the drying conditions on the drying constants and moisture diffusivity during the thin layer drying of figs, *Journal of Food Engineering*, 65(1): pp.449-458.
[23] Goyal, R. K., Kingsley, A. R. P. and Manikantan, M. R. and Ilyas, S. M. 2007. Thin-layer drying kinetics of raw mango slices. *Biosystems engineering*, 95(1): pp.43-49.
[24] Ceylan, I, Aktaş, M and Doğan, H. 2007. Mathematical modeling of drying characteristics of tropical fruits. *Applied Thermal Engineering* 27 (11-12): 1931-1936.

[25] Doymaz, I.2007. Drying behaviour of green beans. *J. of Food Engineering*, 69(1): pp.161–165.
[26] Ozbek, B. and Dadali, G. 2007. Thin-Layer Drying Characteristics and Modelling of Mint Leaves Undergoing Microwave Treatment. *Journal of Food Engineering*, 83, pp.541-549.
[27] Aghbashlo, M., Kianmehr, M.H. and SaminiAkhijahani, H. 2008. Influence of the drying conditions on the effective moisture diffusivity, energy of activation and energy consumption during the thin layer drying of berberic fruit (Berbericdaceae). Energy conversion management, 49(1): pp.2865-2871.
[28] Lopez, A., Iguaz, A., Esnoz, A. and Virseda, P. 2000. Modelling of sorption isotherms of dried vegetable wastes from wholesale market. *Drying Technology*,18(5): pp.985- 994
[29] Kaymak-Ertekin, F. (2002). Drying and Rehydrating Kinetics of Green and Red Peppers. *Journal of Food Science*, 67(1):168-175.
[30] Erbay, Z. and Icier, F. (2010). A review of thin-layer drying of foods: theory, modeling, and experimental results. *Critical Review for Food Science and Nutrition*, 50(5):441–64.
[31] Microsoft Excel 2016. Solver add-ins.
[32] Kantar, Y. M. 2015. Generalized least squares and weighted least squares estimation methods for distributional parameters. *Statistical Journal* 13 (3): 2015, pp.263–282
[33] Demir, V., Gunhan, T., Yagcioglu, A.K. and Degirmencioglu, A. 2004. Mathematical modeling and the determination of some quality parameters of air-dried bay leaves. *Biosystems Engineering* 88(3): pp.325-335.
[34] Erenturk, S., Sahin, M and Guttekin S. (2004) Drying characteristics of clear rosehip. Biosystem Engineering 89(2): 159-166.
[35] Prabhanjan, D. G., Ramaswamy H. S. and G. S. V. Raghavan, 1995. Microwave-assisted convective air drying of thin layer carrots. *Journal of Food Engineering*, 25(1): pp.283–293.
[36] Jaya, S. and H. Das. 2003. A vacuum drying model for mango pulp. *Drying Technology*, 21(1): pp.1215–1234.
[37] Pathere, P. B and Sharma, G. P .2006. Effective moisture diffusivity of onion slices undergoing infrared convective drying. *Biosystem Engineering* 9: pp.285-291
[38] Mohapatra, D., Rao, P. S. 2005. A thin layer drying model of parboiled wheat. *Journal of Food Engineering*,66(4). Pp.513-518.
[39] Doymaz, I. 2005. Drying characteristics and kinetics of okra. *Journal of Food Engineering*, 69(1): pp.275–279.
[40] Maskan, A., Kaya, S. and M. Maskan. 2002. Hot air and sun drying of grape leather (pestil). *Journal of Food Engineering*, 54(1): pp.81–88.
[41] Agarry, S. E. and Owabor, C. N. 2012. Modelling of the drying kinetics of banana under natural convective and forced air drying. Journal of Nigeian Society of Chemical Engineers 27(1): pp. 101-112.

POBOLJŠANJE KVALITETA BANANA POSTUPKOM SUŠENJA: -PRISTUP MATEMATIČKIM MODELOM

Muofunanya F. Umunna[1]; S. A. Adzor[2]; D. F. Ikikiru[1]; O. Nyorere[1]; S. K. Chigbo[3]; E. T. Erokare[1]; A. B. Eke[3]

[1]Department of Agricultural Engineering, Faculty of Engineering, Delta State University of Science and Technology, Ozoro, Nigeria
[2]Department of Materials and Metallurgical Engineering, Faculty of Engineering, Delta State University of Science and Technology, Ozoro, Nigeria
[3]Department of Agricultural and Bioresources Engineering, College of Engineering and Engineering Technology, Micheal Okpara University of Agriculture, Umudike, Nigeria

Apstrakt: Ova studija sistematski je istražila kinetiku solarnog sušenja kriški banana debljine 5 mm, 10 mm i 15 mm na temperaturi od 50°C, 60°C i 70°C.

Koristeći solarnu metodu, proces sušenja je pokazao mehanizam kontrolisan difuzijom, prelazeći sa kratkog perioda konstantne brzine na period preovlađujućeg pada brzine, sve dok se ne postigne ravnotežni sadržaj vlage. Konstanta brzine sušenja (k) pokazuje rastući trend sa povišenom temperaturom, dok je uočena inverzna korelacija sa debljinom preseka kriški, uspostavljajući direktnu i inverznu vezu sa vremenom sušenja i temperaturom, respektivno.

Petnaest tankoslojnih modela sušenja primenjeno je kako bi odgovarali podacima o odnosu vlage (MR).

Model Midilli-Kucuk je pokazao superiorne performanse, pripisane visokoj vrednosti R^2(0,997) i najnižim vrednostima RMSE (0,00228) i X^2 (0,0000132).

Dokazan kao robustan alat, Midilli-Kucuk model je efikasno predvideo kinetiku jednoslojnog sušenja kriški banana, pružajući vredne podatke za dizajn i konstrukcije sušara.

Empirijske jednačine izvedene iz dobijenih podataka omogućavaju ostvarenje predviđanje kinetike sušenja posebno za sušenje kriški banana solarnom metodom.

Ova studija značajno doprinosi razumevanju i optimizaciji procesa sušenja nezrele banane za sušenje, nudeći praktične implikacije za dizajn sušara i poboljšanja obrade.

Ključne reči: *Solarno, sušenje, kinetika, kuvanje, banana, kriške, Midilli-Kucuk, model*

Prijavljen:
***Submitted*:27.03.2024.**
Ispravljen:
***Revised*: 19.05.2024.**
Prihvaćen:
***Accepted*: 29.05.2024.**